



## An Analysis on Radiation Protection Abilities of Different Coloured Obsidians

Zeynep AYGUN<sup>1\*</sup>, Murat AYGUN<sup>2</sup>

<sup>1</sup>Bitlis Eren University, Vocational School of Technical Sciences, 13000, Bitlis, Turkey  
\* Corresponding Author : Email: [zeynep.yarbasi@gmail.com](mailto:zeynep.yarbasi@gmail.com); ORCID: 0000-0002-2979-0283

<sup>2</sup>Bitlis Eren University, Faculty of Science and Arts, Department of Physics, 13000, Bitlis, Turkey  
Email: [maygun@beu.edu.tr](mailto:maygun@beu.edu.tr); ORCID: 0000-0002-4276-3511

### Article Info:

DOI: 10.22399/ijcesen.1076556  
Received : 21 February 2023  
Accepted : 21 June 2023

### Keywords

Radiation attenuation parameters  
Obsidian  
Radiation shielding

### Abstract:

Obsidians are naturally occurring structures which have great interest and are widely used in engineering, nuclear and medical applications. Obsidian, a glassy volcanic rock, is formed as a result of volcanic activity and lava eruptions. In the present study, it is aimed to determine the radiation protection parameters of obsidians with different colours in order to examine the radiation shielding capabilities of the samples. The parameters were determined in the range of 4keV-100 GeV photon energies by using Phy-X/PSD code. In order to make a meaningful analyse for the radiation shielding potentials of the obsidians, the calculated mass attenuation and linear attenuation coefficients were compared with ordinary concrete which can be widely used as shielding material in the nuclear application.

## 1. Introduction

The increase in radiation applications in our daily lives leads to the investigation of radiation protection and therefore alternative radiation protective materials. Many researches were carried out for determining radiation shielding properties of different materials before [1-8]. Obsidian is a natural glassy structure associated to volcanic rocks. Since the glassy volcanic rocks are formed as a result of volcanic activity and lava eruptions, regional differences add various features to the structures. Mexico, Ecuador, Japan, Turkey, Iran, Georgia and Armenia can be considered among the countries with high volcanic activity where the large obsidian deposits are formed. Obsidians can have different colours due to their compositions. Black to brown colours of obsidians are caused by iron and other transition elements of ingredients [9]. Due to the great interest in such structures, obsidians were studied widely before [7,10-13]. Aygun et al. reported the spectroscopic features and radiation shielding potentials of four obsidians from different regions in Turkey [7]. Aygun and Aygun studied radiation protection properties of Rize-İkizdere and Van-Erciş obsidians by Phy-X/PSD code [8]. Build up factors of natural black obsidian ores extracted from Artvin and Van regions [11]. Acıkgöz et al.

studied the physical, structural, and mechanical properties of natural volcanic obsidian glass doped with Er<sub>2</sub>O<sub>3</sub> [12]. Radionuclide and absorption properties of 14 İkizdere obsidian samples were reported and it was concluded that obsidian is a potential material in radiation protection [13].

In this study, it is aimed to calculate radiation shielding parameters of the different coloured obsidians reported by Safaryan et al. [9]. For this purpose, we used a Phy-X/PSD code which can calculate quickly and accurately all specified shielding parameters such as mass attenuation coefficient (MAC), linear attenuation coefficient (LAC), effective atomic number ( $Z_{eff}$ ), half-value layer (HVL), tenth-value layer (TVL), total electronic cross section (ECS), total atomic cross section (ACS), effective electron number ( $N_{eff}$ ), effective conductivity ( $C_{eff}$ ) and fast neutron removal cross section (FNRCs) in photon energies between 4keV and 100GeV [14].

## 2. Material and Methods

The MAC can be determined by the Beer-Lambert given as:

$$I = I_0 e^{-\mu t} \quad (1)$$

$$\mu_m = \frac{\mu}{\rho} = \ln(I_0/I)/\rho t = \ln(I_0/I)/t_m \quad (2)$$

where  $I_0$ ,  $I$ ,  $\rho$  ( $\text{g}/\text{cm}^3$ ),  $\mu_m$  ( $\text{cm}^2/\text{g}$ ),  $\mu$  ( $\text{cm}^{-1}$ ),  $t$  ( $\text{cm}$ ) and  $t_m$  ( $\text{g}/\text{cm}^2$ ) are incident and attenuated photon intensities, density of material, mass, linear attenuation coefficients, the thickness and sample mass thickness (the mass per unit area), respectively.

If the sample has various elements, the total MAC for any compound can be given by Eq. (3) [15];

$$\mu/\rho = \sum_i w_i (\mu/\rho)_i \quad (3)$$

ACS ( $\sigma_a$ ) for any sample can be obtained by the equation;

$$ACS = \sigma_a = \frac{N}{N_A} (\mu/\rho) \quad (4)$$

ECS ( $\sigma_e$ ) is given by the following equation [16]

$$ECS = \sigma_e = \frac{\sigma_a}{Z_{eff}} \quad (5)$$

By using the Equations (4) and (5), we can find the  $Z_{eff}$  of the material as follows;

$$Z_{eff} = \frac{\sigma_a}{\sigma_e} \quad (6)$$

We can calculate  $N_{eff}$  as follows [17],

$$N_{eff} = \frac{\mu_m}{\sigma_e} \quad (7)$$

HVL and TVL are the thickness related parameters. MFP is the average distance at which a photon travels through the material between two interactions. The  $\mu$  is used to calculate the parameters given by

$$HVL = \frac{In(2)}{\mu} \quad (8)$$

$$MFP = \frac{1}{\mu} \quad (9)$$

$$TVL = \frac{In10}{\mu} \quad (10)$$

$C_{eff}$  of the sample can be calculated by the equation [18]:

$$C_{eff} = \left( \frac{N_{eff} \rho e^2 \tau}{m_e} \right) 10^3 \quad (11)$$

FNRCS ( $\sum R$ ) values of the sample can be obtained with the following equation [19,20]:

$$\sum R = \sum_i \rho_i (\sum R / \rho)_i \quad (12)$$

where  $\rho_i$  is the partial density of the material and  $(\sum R / \rho)_i$  is the mass removal cross-section of the  $i^{\text{th}}$  constituent element.

### 3. Results and Discussions

The chemical compositions of different coloured obsidians are given in Table 1 [9]. Variations of the calculated MAC values of the obsidians versus photon energies (4keV-100GeV) are shown in Fig. 1(a). At low energies (1-100keV) where the photoelectric process (PE) is predominant, a decrease in MAC values with increasing energy is observed. In mid-energy region (100keV-5MeV) where the Compton scattering (CS) is dominant, MAC values slightly changed. Above 5 MeV, the Pair production (PP) process starts and an increase in MAC values is obtained with increasing energy [5,21].

**Table 1.** Chemical compositions of black, brown and gray obsidians.

Obsidian	$\text{SiO}_2$	$\text{Al}_2\text{O}_3$	$\text{Fe}_2\text{O}_3$	$\text{CaO}$	$\text{MgO}$	$\text{SO}_3$	$\text{NaO+K}_2\text{O}$
Gray	73.60	14.53	0.69	1.20	0.25	0.31	8.92
Black	74.46	14.20	1.12	1.25	0.28	0.14	8.23
Brown	76.96	13.33	0.96	1.19	0.22	0.16	6.97

LAC is an important parameter for defining the photon-matter interaction. The value of LAC depends on both MAC and density of sample. Variation of the calculated LAC values versus photon energies (4keV-100GeV) is shown in Fig. 1(b). Differences of LAC values are greater than those of MAC values depending on the density effect. It was obtained that the MAC values of the obsidians are very near to each other for the given energies. Obsidians are arranged according to their LAC values as brown>black >gray. Comparison of MAC and LAC values of obsidians with those of ordinary concrete (OC), reported by Bashter [22], to evaluate the shielding potential of the samples is given in Table 2. It can be observed that obsidians show higher protection features than OC. The interaction possibility of per atom and per electron in a unit volume of any material is given by ACS and ECS, respectively. Dependence of ACS and ECS values on incident photon energies are given in Fig. 2(a-b). The obsidian with higher ACS and ECS values can be accepted as better shielding obsidian. According to the obtained results for ACS and ECS parameters of the samples, the shielding potential cannot be determined clearly. The HVL and TVL parameters give the information about the penetration ability of the radiations in materials.

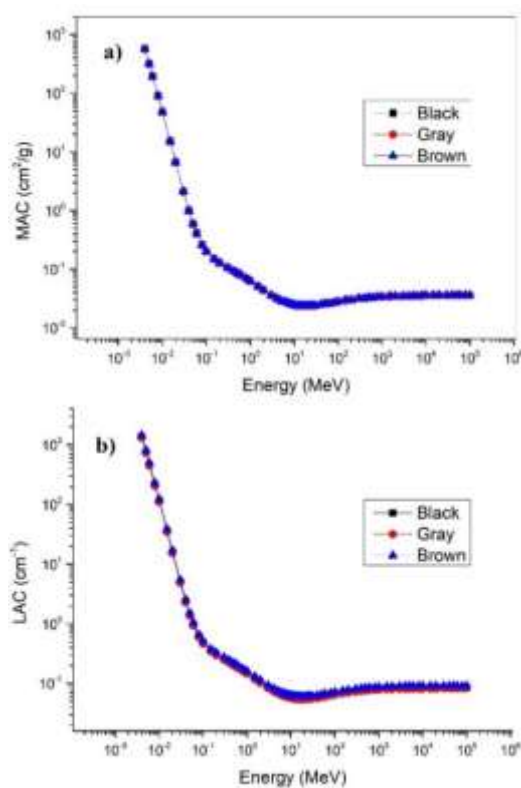


**Figure 1.** The changes of MAC (a) and LAC (b) values as a function of incident photon energy.

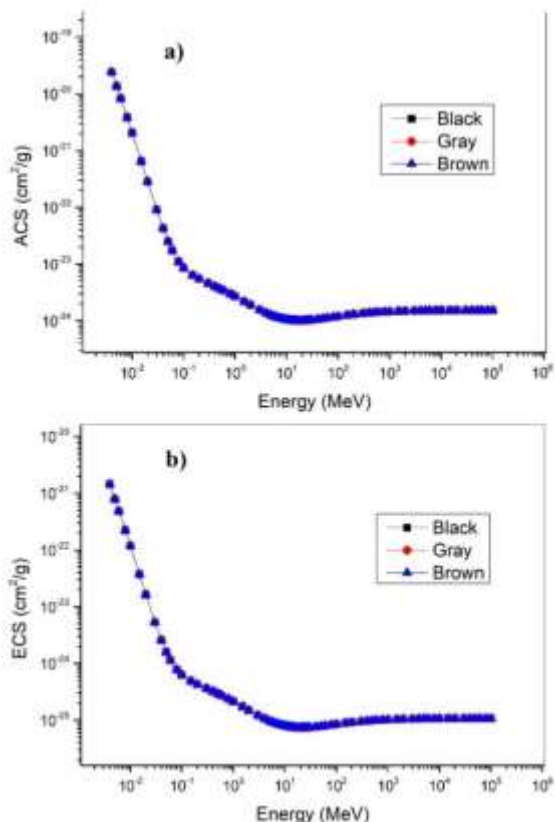


**Figure 2.** The variations of ACS (a) and ECS (b) values as a function of incident photon energy.

HVL, TVL and MFP parameters changing as a function of incident photon energies are given in Fig 3(a-c). In the mid-energy region with CS, most photons are more likely to be scattered. Therefore, their absorption probabilities are lower and hence thicker materials are required and longer MFP would be. As a result of this, an increase in HVL, MFP and TVL values can be observed in the mid-energy region. It is preferred to have low HVL, MFP and TVL values in the high energy regions for better shielding property.

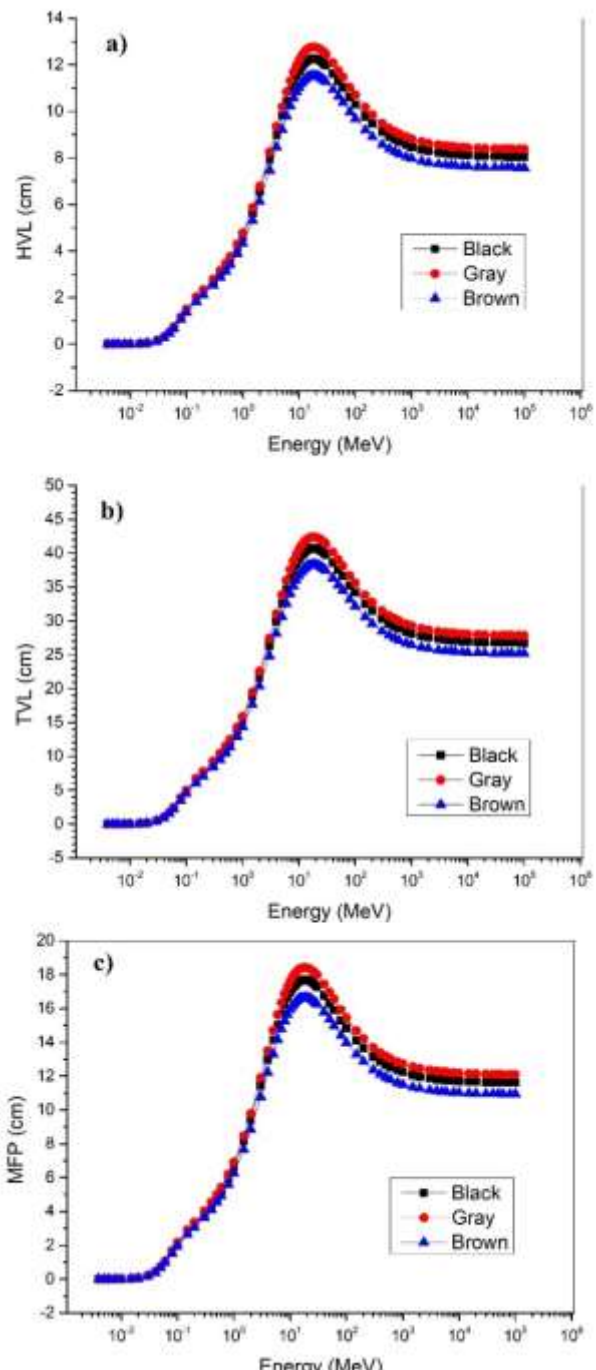


**Figure 3.** Dependence of HVL (a), TVL (b), and MFP (c) values versus incident photon energy.

**Table 2.** MAC and LAC values of the obsidians and OC between the energies of 10keV and 1GeV.

<b>Energy</b>	<b>Black MAC</b>	<b>Black LAC</b>	<b>Brown MAC</b>	<b>Brown LAC</b>	<b>Gray MAC</b>	<b>Gray LAC</b>	<b>OC MAC</b>	<b>OC LAC</b>
<b>MeV</b>	<b>cm<sup>2</sup>/g</b>	<b>1/cm</b>	<b>cm<sup>2</sup>/g</b>	<b>1/cm</b>	<b>cm<sup>2</sup>/g</b>	<b>1/cm</b>	<b>cm<sup>2</sup>/g</b>	<b>1/cm</b>
1.00E-02	48.17	115.6	48.07	122.5	47.80	110.4	22.56	51.89
1.50E-02	15.18	36.44	15.14	38.63	15.05	34.78	7.079	16.28
2.00E-02	6.652	15.96	6.635	16.91	6.594	15.232	3.105	7.142
3.00E-02	2.119	5.087	2.114	5.391	2.101	4.854	1.048	2.410
4.00E-02	0.994	2.386	0.992	2.529	0.986	2.278	0.541	1.245
5.00E-02	0.589	1.413	0.587	1.498	0.584	1.350	0.358	0.824
6.00E-02	0.407	0.977	0.406	1.036	0.405	0.935	0.241	0.555
8.00E-02	0.258	0.619	0.258	0.657	0.257	0.594	0.204	0.469
1.00E-01	0.201	0.481	0.200	0.511	0.200	0.462	0.172	0.396
1.50E-01	0.149	0.357	0.149	0.379	0.149	0.343	0.142	0.328
2.00E-01	0.128	0.308	0.128	0.327	0.128	0.296	0.127	0.292
3.00E-01	0.107	0.258	0.107	0.274	0.107	0.248	0.108	0.249
4.00E-01	0.095	0.228	0.095	0.243	0.095	0.220	0.096	0.222
5.00E-01	0.086	0.208	0.087	0.221	0.086	0.200	0.088	0.202
6.00E-01	0.080	0.191	0.080	0.204	0.080	0.184	0.079	0.183
8.00E-01	0.070	0.168	0.070	0.178	0.070	0.161	0.071	0.164
1.00E+00	0.063	0.151	0.063	0.160	0.063	0.145	0.064	0.147
1.50E+00	0.051	0.123	0.051	0.130	0.051	0.118	0.052	0.120
2.00E+00	0.044	0.106	0.044	0.113	0.044	0.102	0.045	0.103
3.00E+00	0.036	0.087	0.036	0.093	0.036	0.084	0.036	0.084
4.00E+00	0.032	0.077	0.032	0.082	0.032	0.074	0.031	0.073
5.00E+00	0.029	0.071	0.029	0.075	0.029	0.068	0.028	0.066
6.00E+00	0.028	0.067	0.028	0.071	0.028	0.064	0.026	0.061
8.00E+00	0.026	0.062	0.026	0.065	0.026	0.059	0.024	0.056
1.00E+01	0.025	0.059	0.025	0.063	0.025	0.057	0.022	0.052
1.50E+01	0.024	0.057	0.024	0.060	0.024	0.055	0.021	0.048
2.00E+01	0.024	0.057	0.024	0.060	0.024	0.054	0.019	0.043
5.00E+01	0.026	0.061	0.026	0.065	0.026	0.059	0.021	0.048
1.00E+02	0.028	0.067	0.028	0.072	0.028	0.065	0.022	0.052
5.00E+02	0.033	0.079	0.033	0.084	0.033	0.076	0.026	0.061
1.00E+03	0.034	0.082	0.034	0.087	0.034	0.079	0.027	0.063

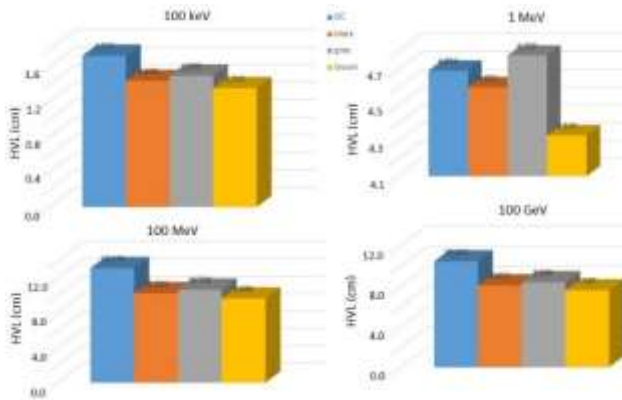


**Figure 4.** HVL values of obsidians and OC for 100 keV, 1 MeV, 100 MeV and 100 GeV.

It was obtained that HVL, MFP and TVL values of the studied obsidians are brown<black<gray. Comparison of HVL values of obsidians and OC for 100 keV, 1 MeV, 100 MeV and 100 GeV can be seen in Fig. 4. The energy dependence of  $Z_{\text{eff}}$ ,  $N_{\text{eff}}$  and  $C_{\text{eff}}$  are given in Fig. 5(a-c). In the low energy region due to the photoelectric effect, maximum  $Z_{\text{eff}}$  values were obtained. By increasing energy, these values decreased sharply. The values gradually increased and be stable in high energies. It was seen that  $Z_{\text{eff}}$  values of the obsidians are very close.  $N_{\text{eff}}$  is one of the parameter that represents the effective conductivity of the compound depending on the excitatory photon energy [17]. As shown in Fig. 5, the change of the  $N_{\text{eff}}$  values on the incident photon energies is similar with the change of  $Z_{\text{eff}}$  values. The interactions between photons and material with PE, CS, and PP interaction processes can change the number of free electrons in the material. The order of  $C_{\text{eff}}$  values in the given energies is brown>black>gray.

Fast neutron attenuation ability of the samples is also determined by Phy-X/PSD. FNRCs values of black, gray and brown obsidians are obtained as 0.073, 0.070 and 0.078, respectively. It is obtained that brown obsidian has higher neutron attenuation among the obsidians. It can be seen that FNRCs values of the obsidians are higher than the other reported samples (Fig. 6).

#### 4. Conclusions

In this study, radiation-matter interaction parameters of colored obsidians were obtained to determine the radiation shielding capabilities. For this purpose, the MAC, LAC, HVL, TVL, MFP, ACS, ECS,  $Z_{\text{eff}}$ ,  $N_{\text{eff}}$ ,  $C_{\text{eff}}$  and FNRCs parameters of the present samples were calculated by Phy-X / PSD code in the range of 4keV-100GeV. According to the obtained results,

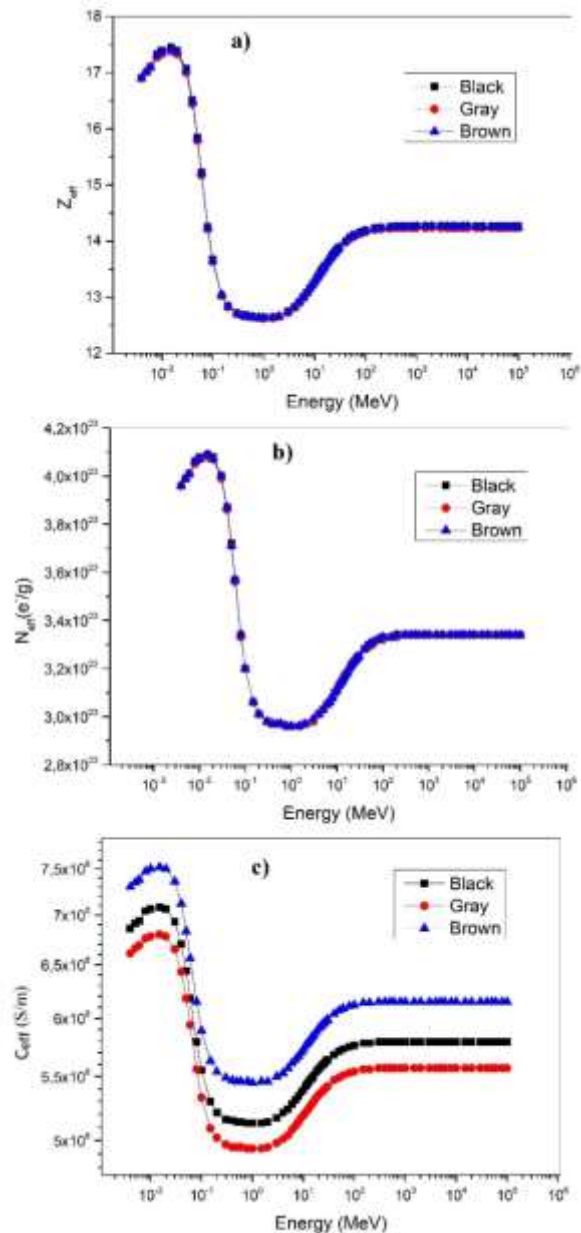


**Figure 5.** The changes of  $Z_{\text{eff}}$  (a)  $N_{\text{eff}}$  (b) and  $C_{\text{eff}}$  (c) values as a function of incident photon energy.

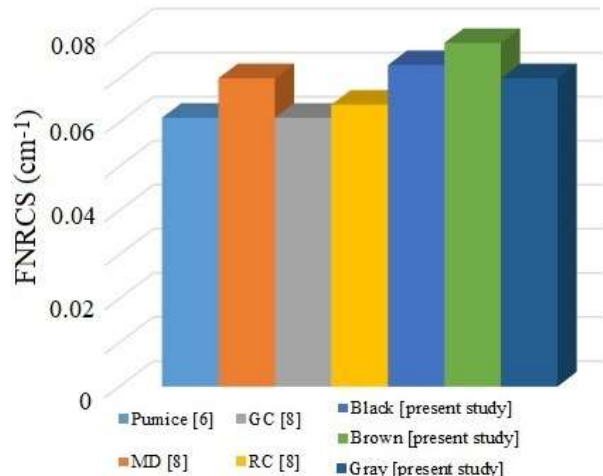


**Figure 6.** FNRCs values of the obsidians and previously reported materials.

although, some of the parameters of the studied obsidians have near values, it was concluded that brown obsidian has the highest shielding potential compared to others. FNRCS is also greater for brown obsidian than the others, therefore fast neutron attenuation potential is higher for brown sample.

## Author Statements:

- **Ethical approval:** The conducted research is not related to either human or animal use.
- **Conflict of interest:** The authors declare that they have no known competing financial interests or personal relationships that could have appeared to influence the work reported in this paper
- **Acknowledgement:** The authors declare that they have nobody or no-company to acknowledge.
- **Author contributions:** The authors declare that they have equal right on this paper.
- **Funding information:** The authors declare that there is no funding to be acknowledged.
- **Data availability statement:** The data that support the findings of this study are available on request from the corresponding author. The data are not publicly available due to privacy or ethical restrictions.

## References

- [1] Akkurt, I., Akyıldırım, H., Mavi, B., Kılıncarslan, S., Basyigit, C., (2010). Radiation shielding of concrete containing zeolite. *Radiat Measur.* 45:827–830. DOI: 10.1016/j.radmeas.2010.04.012
- [2] Akkurt, I., Tekin, H.O. (2020). Radiological parameters of bismuth oxide glasses using the Phy-X/PSD software. *Emerging Mater. Res.* 9:1020-1027. DOI: 10.1680/jemmr.20.00209
- [3] Alim, B. (2020). A comprehensive study on radiation shielding characteristics of Tin Silver, Manganin R, Hastelloy B, Hastelloy X and Dilver P alloys. *Appl. Phys. A* 126:262. DOI:10.1007/s00339-020-3442-7
- [4] Gur, A., Artig, B., Çakır, T. (2017). Photon attenuation properties of concretes containing magnetite and limonite ores. *Physicochem. Probl. Miner. Process.* 53(1):184–191. DOI: 10.5277/ppmp170115
- [5] Kurudirek, M., Türkmen, I., Özdemir, Y. (2009). A study of photon interaction in some building materials: High-volume admixture of blast furnace slag into Portland cement. *Radiat. Phys. Chem.* 78:751–759. DOI: 10.1016/j.radphyschem.2009.03.070
- [6] Aygun, Z., Aygun, M. (2022). A study on usability of Ahlat ignimbrites and pumice as radiation shielding materials, by using EpiXS code. *Inter. J. Environ. Sci. Tech.* 19: 5675–5688. DOI: 10.1007/s13762-021-03530-9
- [7] Aygun, Z., Yarbasi, N., Aygun, M. (2021). Spectroscopic and radiation shielding features of Nemrut, Pasinler, Sarıkamış and İkizdere obsidians in Turkey: Experimental and theoretical study. *Ceramics Inter.* 47:34207–34217. DOI: 10.1016/j.ceramint.2021.08.330
- [8] Aygun, Z., Aygun, M., Yarbasi, N. (2021). A study on radiation shielding potentials of green and red clayey soils in Turkey reinforced with marble dust and waste tire. *J. New Results Sci.* 10:46-59. DOI: [10.54187/jnrs.986038](https://doi.org/10.54187/jnrs.986038)
- [9] Safaryan, A., Sarkisyan, T., Paytyan, T., Baghdagulyan, A. (2020). *The origin and bloating of the obsidian.* E3S Web of Conferences 175:12020. DOI: 10.1051/e3sconf/202017512020
- [10] Aygun, Z., Aygun, M. (2022). Theoretical evaluation on radiation shielding features of Van-Ercis, and Rize-İkizdere (Türkiye) obsidians by using Phy-X/PSD code. *Sigma J. Eng. Nat. Sci.* 40(4): 845–854. DOI: 10.14744/sigma.2022.00100
- [11] Küçük, N., Gezer O. (20170). Doğal Siyah Obsidyen Cevherleri İçin Yıgilma Faktörlerinin Belirlenmesi. *AKU J. Sci. Eng.* 17(3): 872–880. DOI: 10.5578/fmbd.66223
- [12] Acikgoz, A., Ceyhan, G., Aktas, B., Yalcin, S., Demircan, G. (2021). Luminescent, structural and mechanical properties of erbium oxide doped natural obsidian glasses. *J. Non-Crystall. Solids* 572:121104. DOI:10.1016/j.jnoncrysol.2021.121104
- [13] Duran, S.U., Küçükömeroğlu, B., Çiriş, A., Ersoy, H. (2022). Gamma-ray absorbing characteristic of obsidian rocks as a potential material for radiation protection. *Radiat. Phys. Chem.* 199:110309. DOI:[10.1016/j.radphyschem.2022.110309](https://doi.org/10.1016/j.radphyschem.2022.110309)
- [14] Sakar, E., Özpolat, Ö.F., Alim, B., Sayyed, M.I., Kurudirek, M. (2020). Phy-X / PSD: Development of a user friendly online software for calculation of parameters relevant to radiation shielding and dosimetry. *Radiat Phys Chem,* 166:1-12. DOI: 10.1016/j.radphyschem.2019.108496
- [15] Jackson, D.F., Hawkes, D.J. (1981). X-ray attenuation coefficients of elements and mixtures. *Phys. Reports* 70:169–233. DOI: 10.1016/0370-1573(81)90014-4
- [16] Han, I., Demir, L. (2009). Determination of mass attenuation coefficients, effective atomic and electron numbers for Cr, Fe and Ni alloys at different energies. *Nucl Instr Methods Phys Res Sec B* 267:3–8. DOI: 10.1016/j.nimb.2008.10.004
- [17] Han, I., Demir, L. (2009). Studies on effective atomic numbers, electron densities from mass attenuation coefficients in  $TixCo_{1-x}$  and  $CoxCu_{1-x}$  alloys. *Nucl Instr Methods B* 267:3505–3510. DOI: 10.1016/j.nimb.2009.08.022
- [18] Manjunatha, H.C. (2017). A study of gamma attenuation parameters in poly methyl methacrylate and Kapton. *Radiat Phys Chem,* 137:254–259. DOI: 10.1016/j.radphyschem.2016.01.024
- [19] Şakar, E. (2020). *Radiat. Phys. Chem.* 172:1-13. DOI: 10.1016/j.radphyschem.2020.108778
- [20] Wood, J. (2013). *Computational methods in reactor shielding*, Elsevier.

- [21] Alim, B. (2020). Determination of Radiation Protection Features of the Ag<sub>2</sub>O Doped Boro-Tellurite Glasses Using Phy-X / PSD Software. *J. Ins. Sci. Tech.* 10(1):202-213. DOI: 10.21597/jist.640027
- [22] Bashter, I.I. (1997). Calculation of radiation attenuation coefficients for shielding concretes. *Annl. Nucl. Energy* 24(17):1389-1401. DOI: 10.1016/S0306-4549(97)00003-0